Supporting Information

Fabrication of Core-shell like structured Polymeric ionic liquid hybrid catalysts for aqueous reactions

Xiaotong Lu [a], Shengnan Li [a], Chengyao Zhao[a], Yujing Liu [a,b], Zhongqiu Liu [a,b], Anguo Ying [a,b,*]

[a] *School of Chemistry and Chemical Engineering, Qufu Normal University, P. R. China*

[b] *Key Laboratory of Life-Organic Analysis of Shandong Province, School of Chemistry and Chemical Engineering, Qufu Normal University, P. R. China*

E-mail addresses: yinganguo@163.com (A. Ying).

1. Experimental

1.1 Preparation of the ILs

Synthesis of hydrophilic ionic liquids (MIE ILs). (1) Synthesis of tosylated mono-methoxytriethylene glycol (tosylated m-TEG). A solution of triethylene glycol monomethyl ether (10.324 g, 62.88 mmol, 1.2eq) and p-Toluenesulfonyl chloride (10.01 g, 52.4 mmol, 1eq) in DCM (100 mL) was cooled in an ice bath at N_2 atmosphere, and then triethylamine was added drop by drop to the solution slowly. The solution was stirred at room temperature for 12 h and then removed insoluble matter by filtration. The remaining solution was washed by deionized water (3 x 100 mL) and saturated $NaHCO_3$ (100 mL) in turn and dried over $MgSO_4$, and the pure product was obtained by column chromatography (PE: EA=1:3), eluted purified product 11.46 g, Yield 68.6%.

(2) Synthesis of 3-(2-(2-(2-methoxyethoxy)ethoxy)ethyl)-1-vinyl-1H-imidazol-3-ium 4-methylbenzenesulfonate (MIE-ILs). Tosylated m-TEG (2 mmol, 0.64 g) was added to the mixture of vinylimidazole (2 mmol, 0.18 g) and K_2CO_3 (2 mmol, 0.276 g) in dry CH_3CN (10 mL) and stirred at 60 °C for 24 h at N_2 atmosphere. The reaction was cooled to room temperature. The solid material was separated by filtration and washed by H_2O and EtOAc and obtained the MIE-ILs by reduced pressure distillation. The structure and chemical composition of MIE-ILs were identified by ^1H NMR spectrum (see Figure S1). ^1H NMR (500 MHz, DMSO): δ (ppm): 7.68-7.66 (d, 1H,), 7.58-7.55 (d, 2H,), 7.49-7.51 (d, 1H), 5.67-5.72 (m, 1H), 5.34-5.31 (m, 1H), 4.28-4.34 (m, 2H), 3.77-3.83 (m, 2H), 3.44-3.62 (m, 10H), 3.25 (s, 3H).

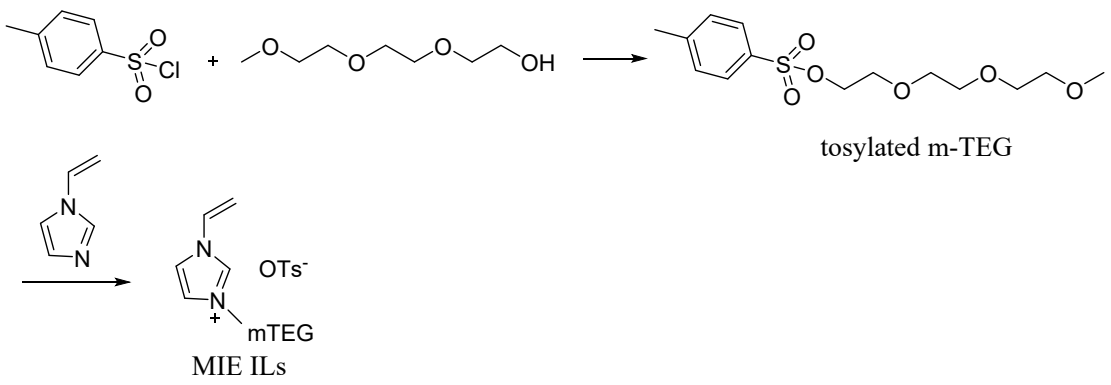

Scheme S1. Synthesis of the SPA monomer

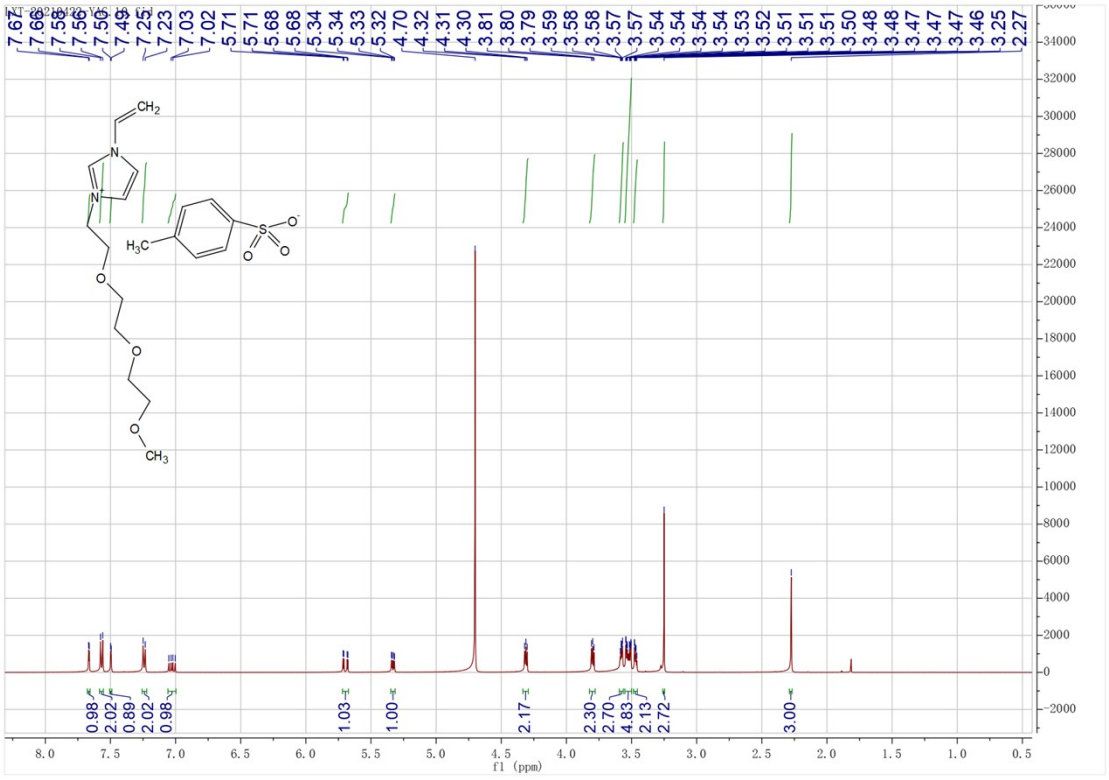

Fig. S1 ^{1}H NMR of the MIE-ILs monomer

1.2 Equilibrium adsorption isotherms of MIE@Pd/SiNP-CPDB and MIE@Pd/SiNP-CPDB(no PTES) nanoparticles

50 μL of styrene were added to 5 mL of water containing 20 mg of different nanoparticles at 303 K, 308 K, 313 K, and 318 K respectively. The adsorption was

carried out in a sealed glass vial by equilibrating the mixture for 1 h on a magnetic stirring apparatus. After adsorption, the materials were directly removed from solution by filtration. The styrene was extracted by ethyl acetate for 3 times. Then, the amount of styrene was measured with an internal standard method by gas chromatography. The adsorption enthalpy was calculated following the derivative Clausius-Clapeyron equation, $\ln Ce = \Delta H/(RT) + \ln K$, where ΔH is the adsorption enthalpy (KJ/mol), T is the absolute temperature (K), Ce represent the initial and equilibrium concentrations (mg/g), R is the ideal gas constant [8.314 J/(mol·K)], and K is a constant.

1.3 Characterizations of the nMIE@Pd@SiNP-CPDB catalysts

XRD patterns of the nMIE@Pd/SiNP-CPDB catalysts were determined with a PANalytical Empyrean X-ray diffractometer (Netherlands). The scanning speed was 10° min^{-1} from 2θ = 10° to 90°. The ICP-OES and fourier transform infrared (FTIR) spectra of the samples were recorded on a Thermo Fisher Scientific (US). XPS analysis of the surface microstructure information of the samples were performed with a Thermo Kalpha X-ray photo-electron spectrometer (US). The organic elements analysis of the catalysts samples were tested by means of a Elementar Vario EL (Germany). The scanning electron microscope (SEM) of the samples were performed with a Sigma 500VP (Carl Zeiss AG) and transmission electron microscope (TEM) of the samples were observed with a JEM-2100PLUS (80-200kV, Japan). N2 adsorption-desorption isotherms of the samples were recorded with a KuboX1000 series surface area and porosity analyzer (CN). The thermo gravimetric analysis (TGA) of the samples were performed with a TA system (NETZSCH, Germany). The

conversion of various substrates was determined by GC-MS, nitrogen was used as the carrier gas with a flow of 30 mL·min^{-1}, injector temperature and detector temperature were 250 °C, column temperature was programmed from 50 to 280 °C with 5 °C·min^{-1}.

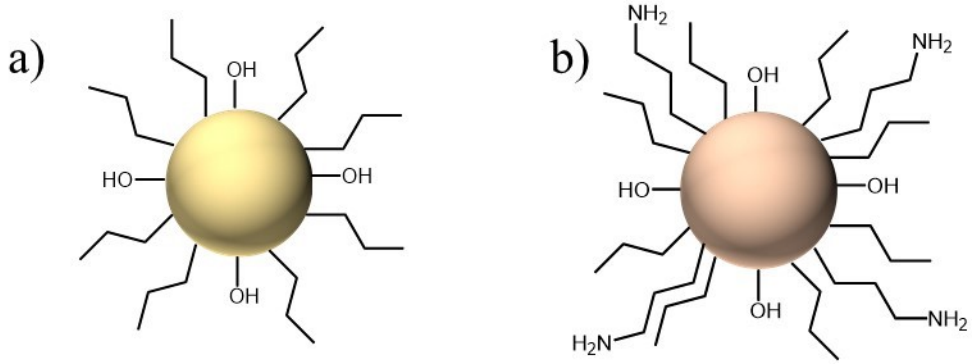

Fig. S2 Chemical structure schematic of a) Hydrophobic silicon core and b) Ammoniated hydrophobic silicon cores.

Table S1

Textural parameters of the prepared organic-inorganic hydrophobic silica cores

Entry	OSi/Si (Mol)	BET surface area (m^2 g^{-1})	Pore volume (cm^3 g^{-1})	Average pore size (nm)
1	1- 0	552	2.11	4.68
2	1- 0.1	896	0.88	2.80
3	1- 0.2	804	0.79	2.85
4	1- 0.3	859	0.70	2.87
5	1- 0.4	836	0.67	2.85
6	1- 0.5	850	0.63	2.86

Table S2

Textural parameters of Pd/SiNP-CPDB, MIE@Pd/SiNP-CPDB, 2MIE@Pd/SiNP-CPDB and 3MIE@Pd/SiNP-CPDB.

Entry	Sample	BET surface area (m^2 g^{-1})	Pore volume (cm^3 g^{-1})	Average pore size (nm)
1	Pd/SiNP-CPDB	713	0.65	2.81
2	MIE@Pd/SiNP-CPDB	574	0.55	2.74
3	2MIE@Pd/SiNP-CPDB	489	0.41	2.50
4	3MIE@Pd/SiNP-CPDB	409	0.31	2.41

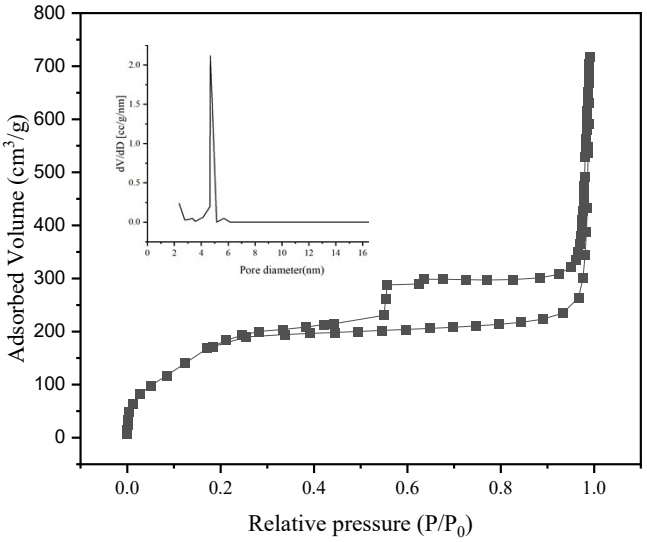

Figure S3. N_2 adsorption-desorption isotherm and pore size distribution of SiNP-CPDB with OSi/Si molar ratio of 0/1.

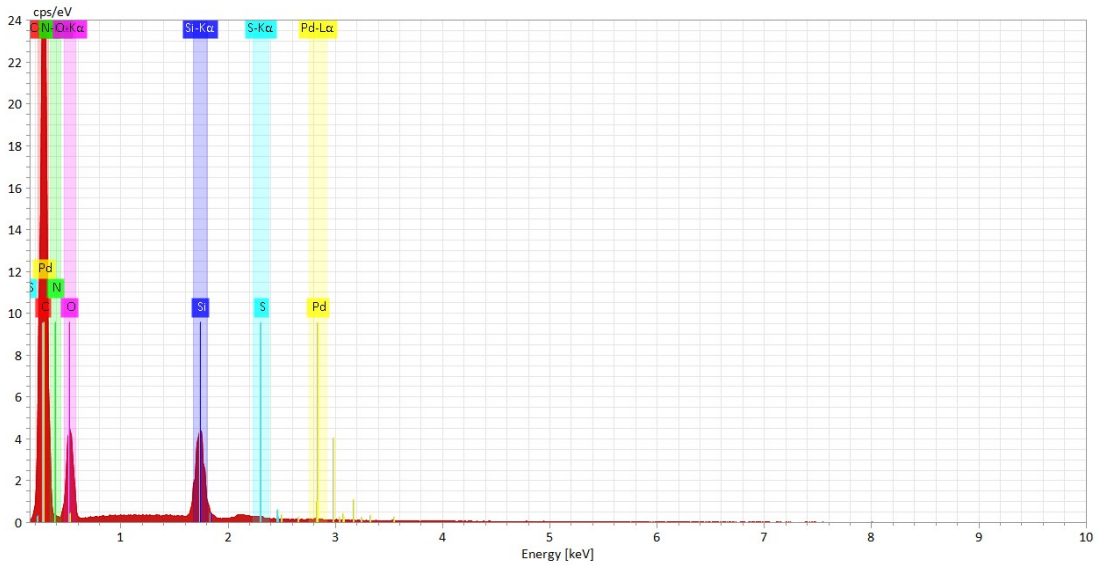

87

88 **Figure S4**. EDX spectrum of the MIE@Pd/SiNP-CPDB catalyst.

89

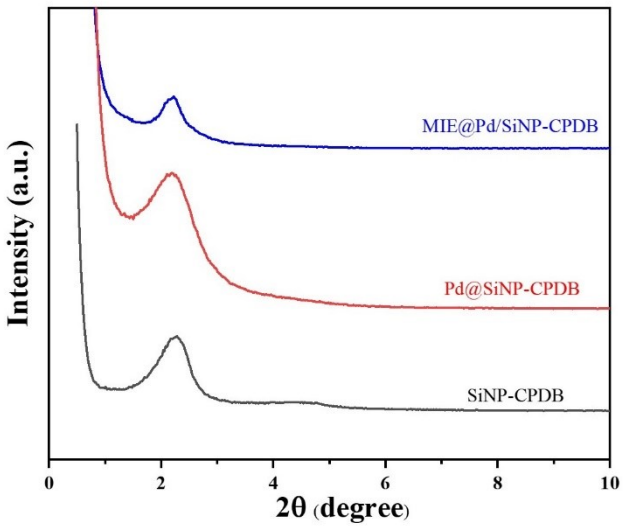

90

91 **Figure S5.** Low angle XRD of SiNP-CPDB, Pd/SiNP-CPDB and MIE@Pd/SiNP-
92 CPDB.

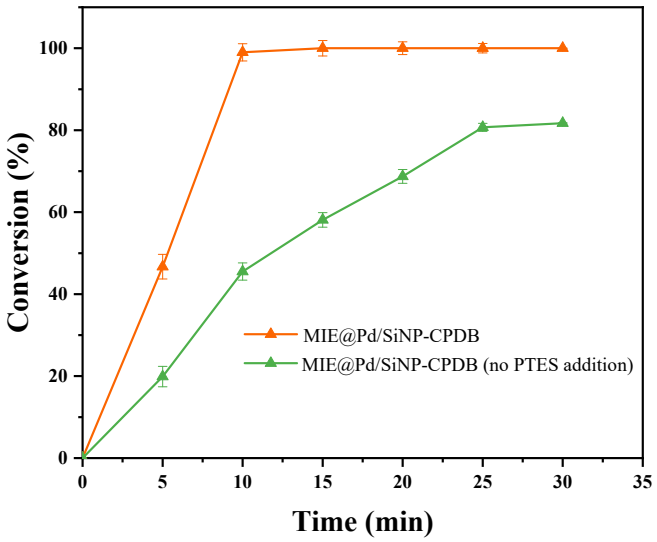

Figure S6. Hydrogenation of styrene catalyzed by MIE@Pd/SiNP-CPDB and MIE@Pd/SiNP-CPDB (no PTES addition).

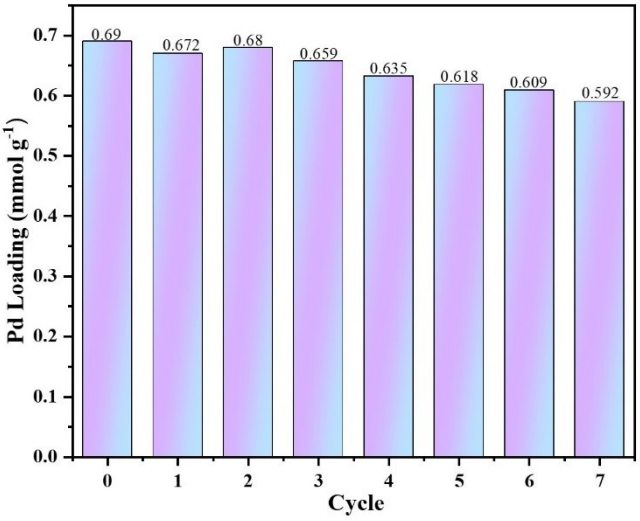

Figure S7. The Pd loading of MIE@Pd/SiNP-CPDB after every cycle detected by ICP-OES.

Table S3. The catalytic effect of different catalysts on styrene hydrogenation.

	Reaction	Reaction	Yield

Entry	catalyst	Time (min)	condition	(Con.) (%)	Ref.
1	MIE@Pd/SiNP-CPDB	10	25 °C 101 kPa	100	This work
2	[C4AzoC2DMEA]Br/Pd@SM	40	25 °C 101 kPa	>99	1
3	Pd/MSS-C20	35	40 °C 0.35 MPa	89	2
4	Pd/SN-ON	90	40 °C 0.35 MPa	>99	3
5	Pd/PEG4000	90	25 °C 101 kPa	60	4

102

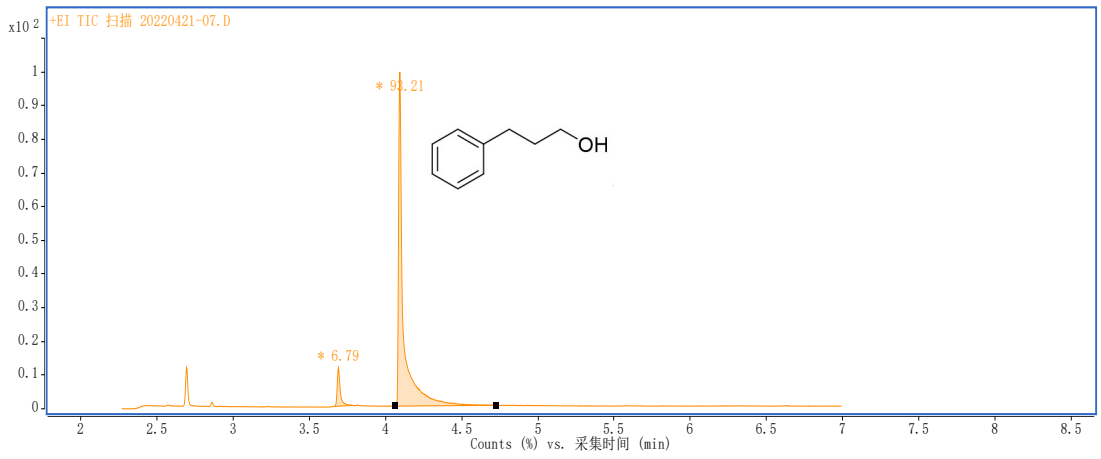

103

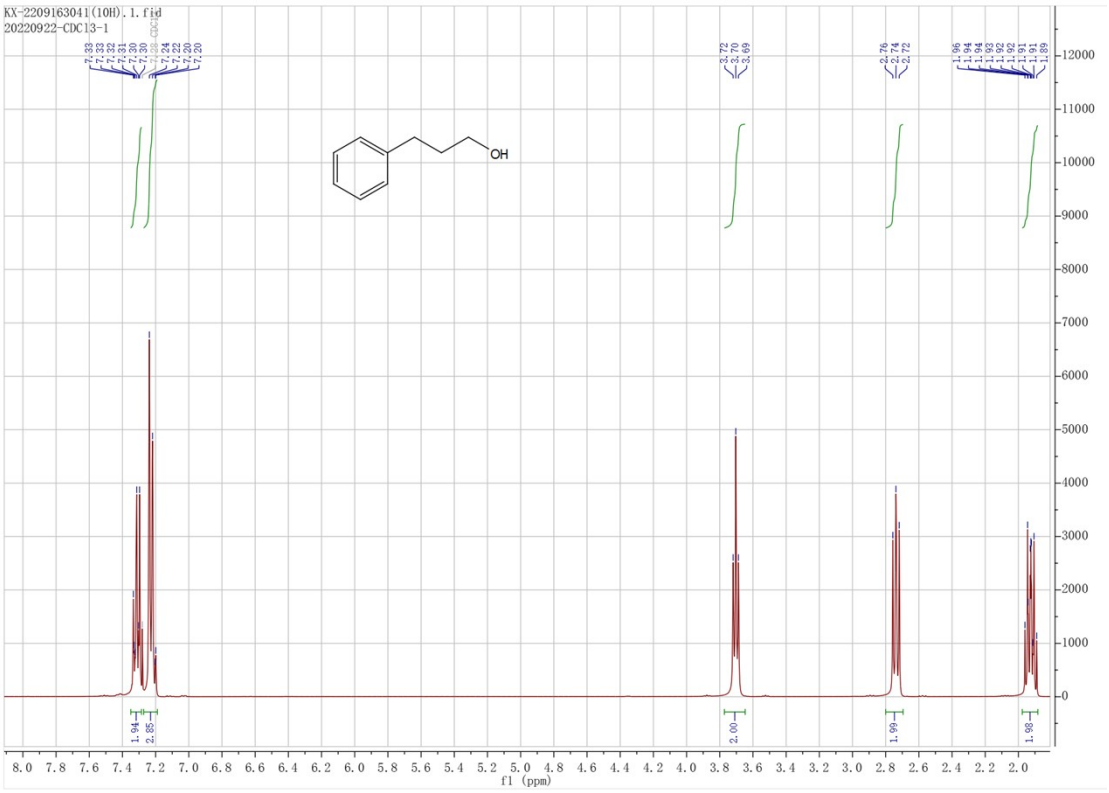

104

105 ^{1}H NMR (500 MHz, $CDCl_3$): δ (ppm): 7.33-7.30 (m, 2H,), 7.24-7.20 (m, 3H,), 3.72-

106 3.69 (t, 2H), 2.76-2.72 (t, 2H), 1.96-1.89 (m, 2H).

107 **Figure S8.** The GC-MS and ^{1}H NMR spectrum of the hydrogenation results (table 2

108 of main text, entry 1).

109

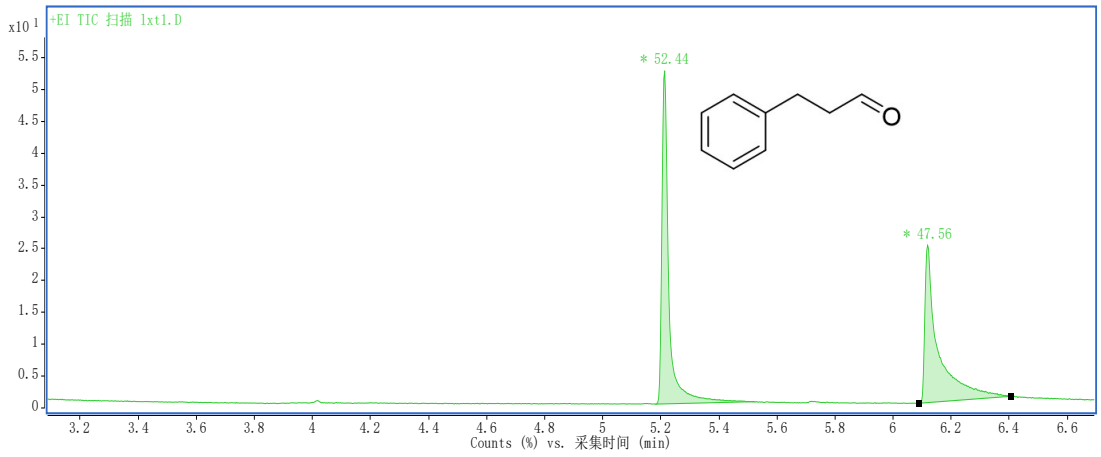

110

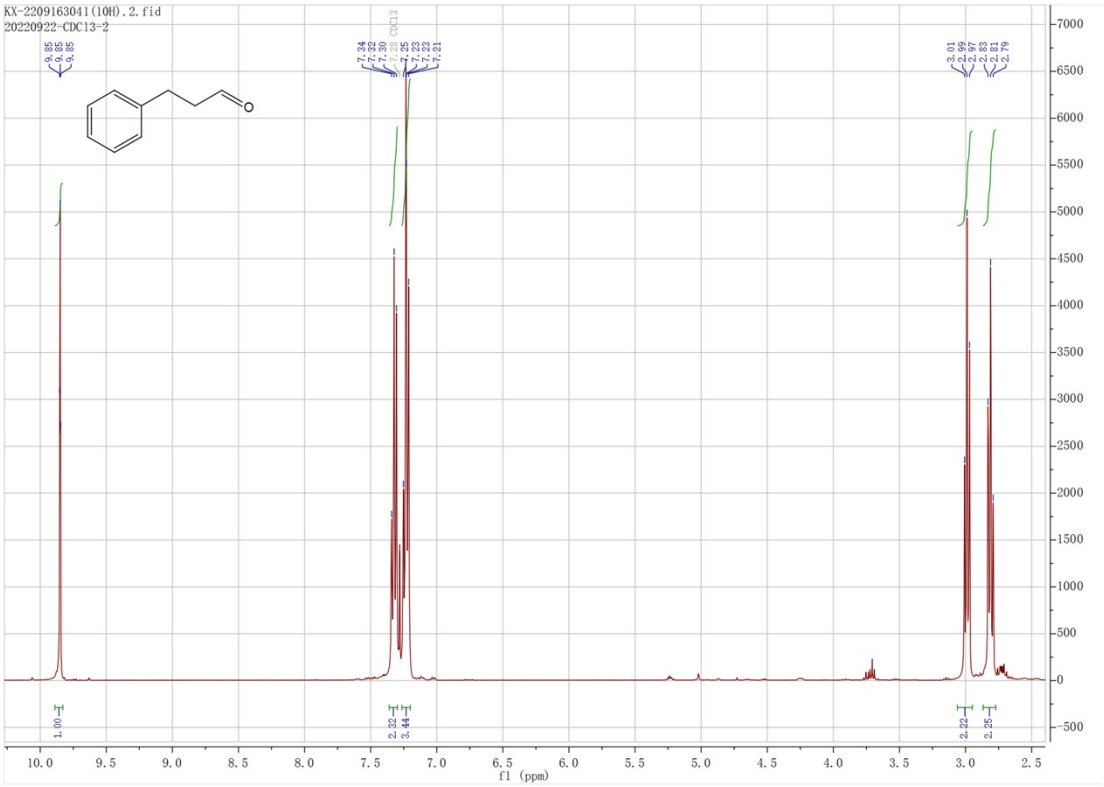

111

112 ^{1}H NMR (500 MHz, $CDCl_3$): δ (ppm): 9.85 (s,1H) 7.34-7.30 (m, 2H,), 7.25-7.21 (m,

113 3H,), 3.01-2.97 (t, 2H), 2.83-2.79 (t, 2H).

114 **Figure S9.** The GC-MS and ^{1}H NMR spectrum of the hydrogenation results (table 2

115 of main text, entry 2).

116

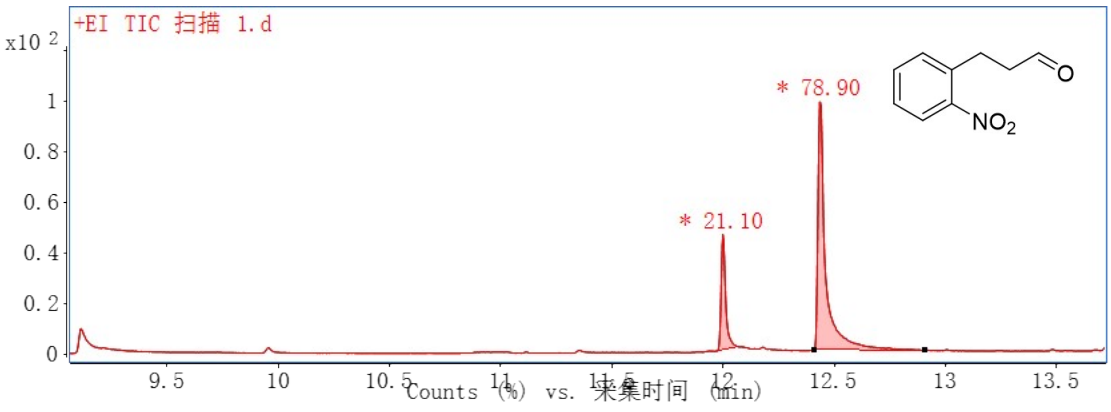

117

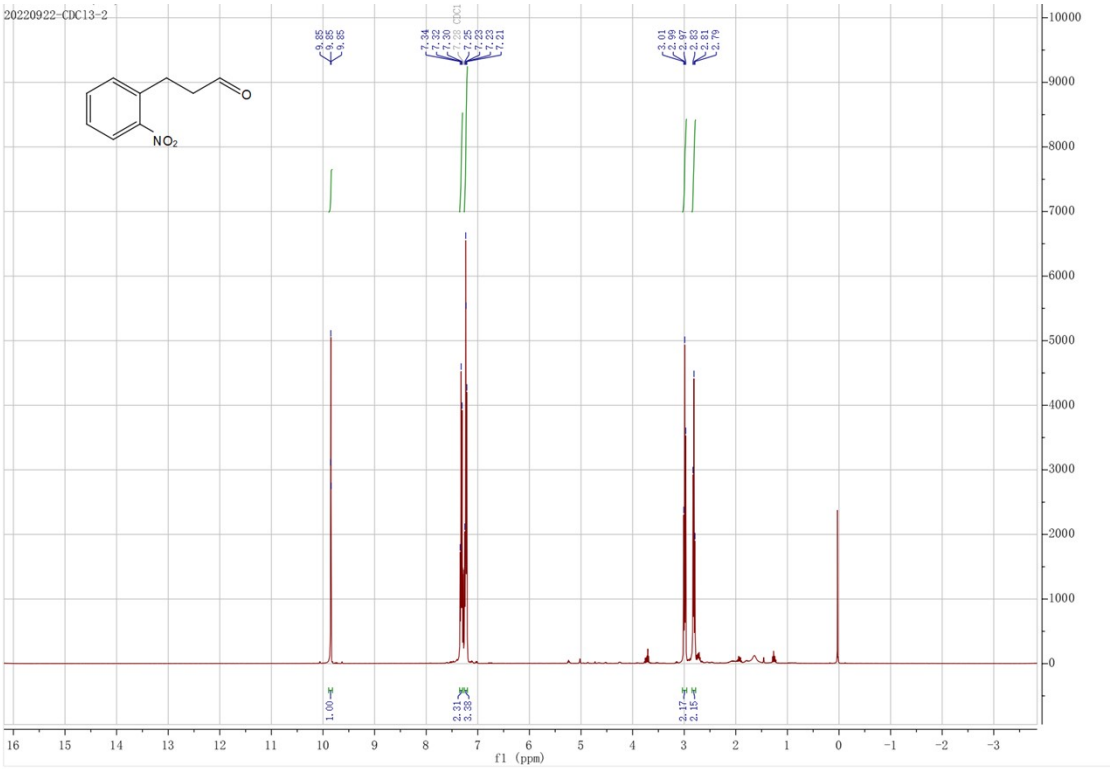

118

119 ^{1}H NMR (500 MHz, $CDCl_3$): δ (ppm): 9.85 (s,1H) 7.34-7.30 (m, 2H,), 7.25-7.21 (m,

120 3H,), 3.01-2.97 (t, 2H), 2.83-2.79 (t, 2H).

121 **Figure S10.** The GC-MS and ^{1}H NMR spectrum of the hydrogenation results (table 2

122 of main text, entry 3).

123

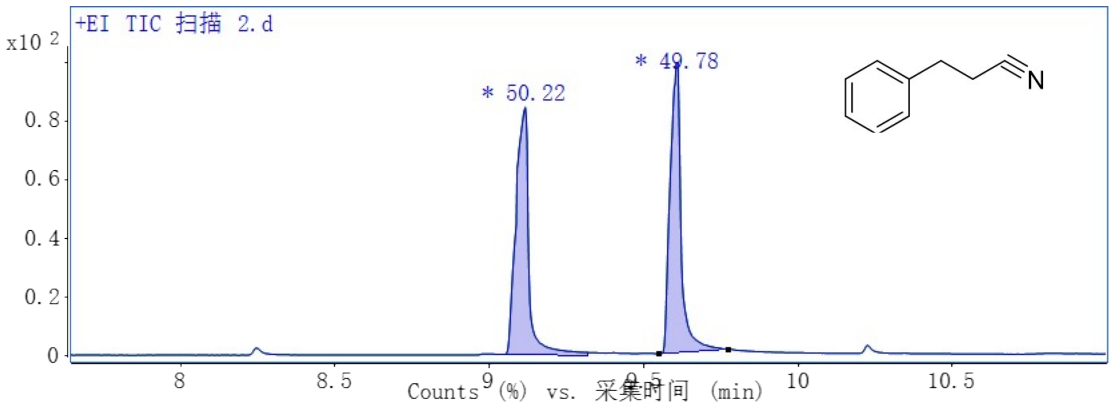

124

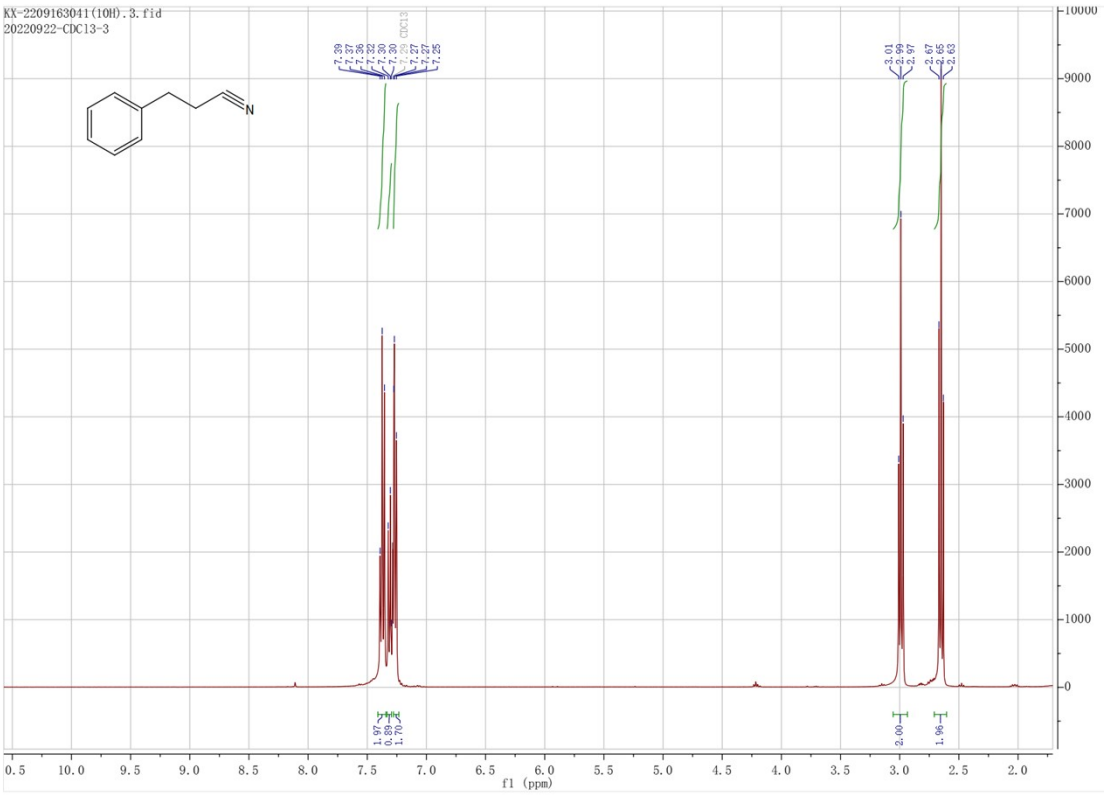

125

126 ^{1}H NMR (500 MHz, $CDCl_3$): δ (ppm): 7.39-7.32 (M, 2H)， 7.30 (S, 1H), 7.27-7.25

127 (t, 2H,), 3.01-2.97 (t, 2H), 2.67-2.63 (t, 2H).

128 **Figure S11.** The GC-MS and ^{1}H NMR spectrum of the hydrogenation results (table 2

129 of main text, entry 4).

130

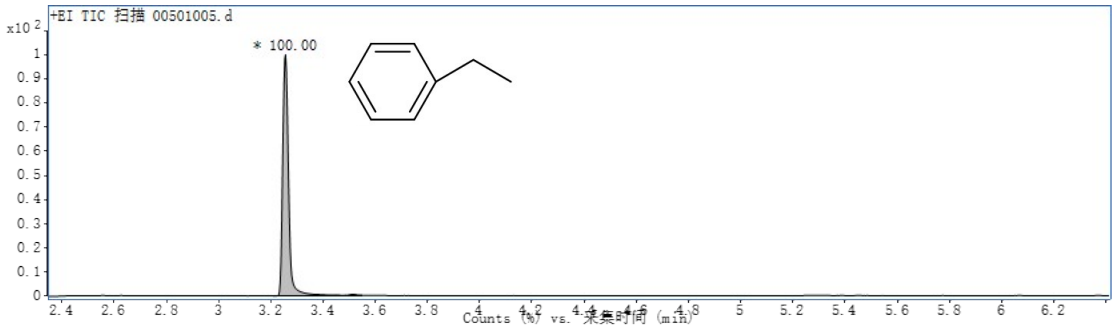

131

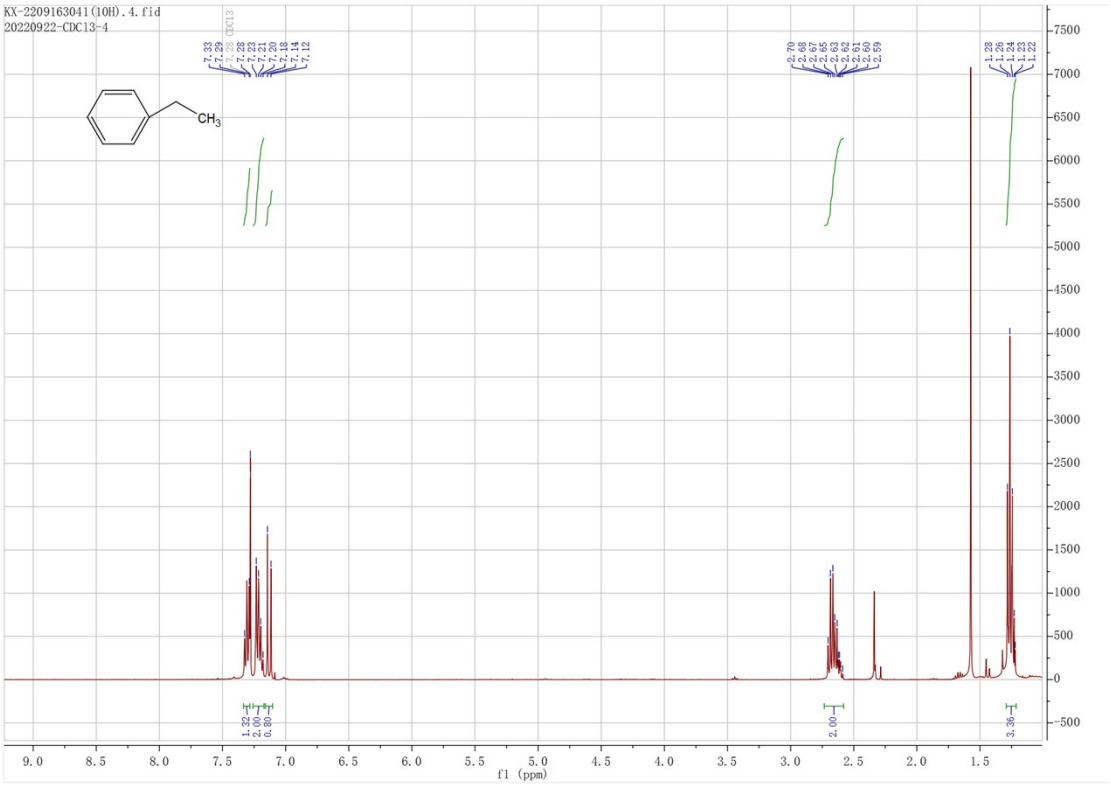

132

133 ^{1}H NMR (500 MHz, $CDCl_3$): δ (ppm): 7.33-7.29 (d, 2H), 7.28-7.12 (m, 3H), 2.70-

134 2.59 (m, 2H), 1.28-1.22 (m, 3H).

135 **Figure S12.** The GC-MS and ^{1}H NMR spectrum of the hydrogenation results (table 2

136 of main text, entry 5).

137

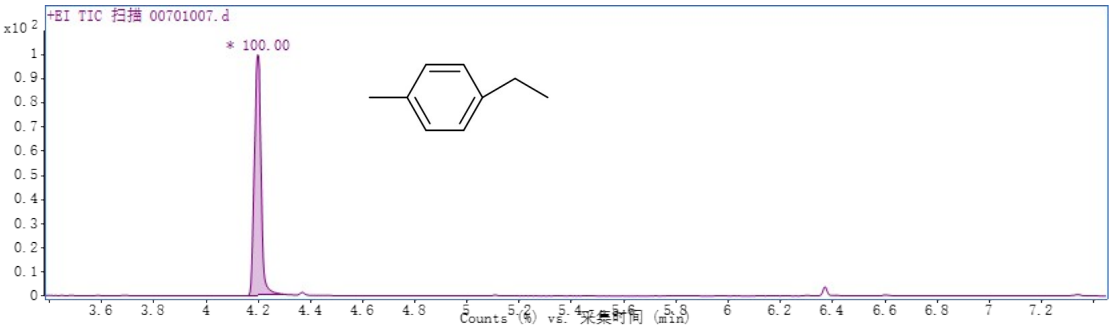

138

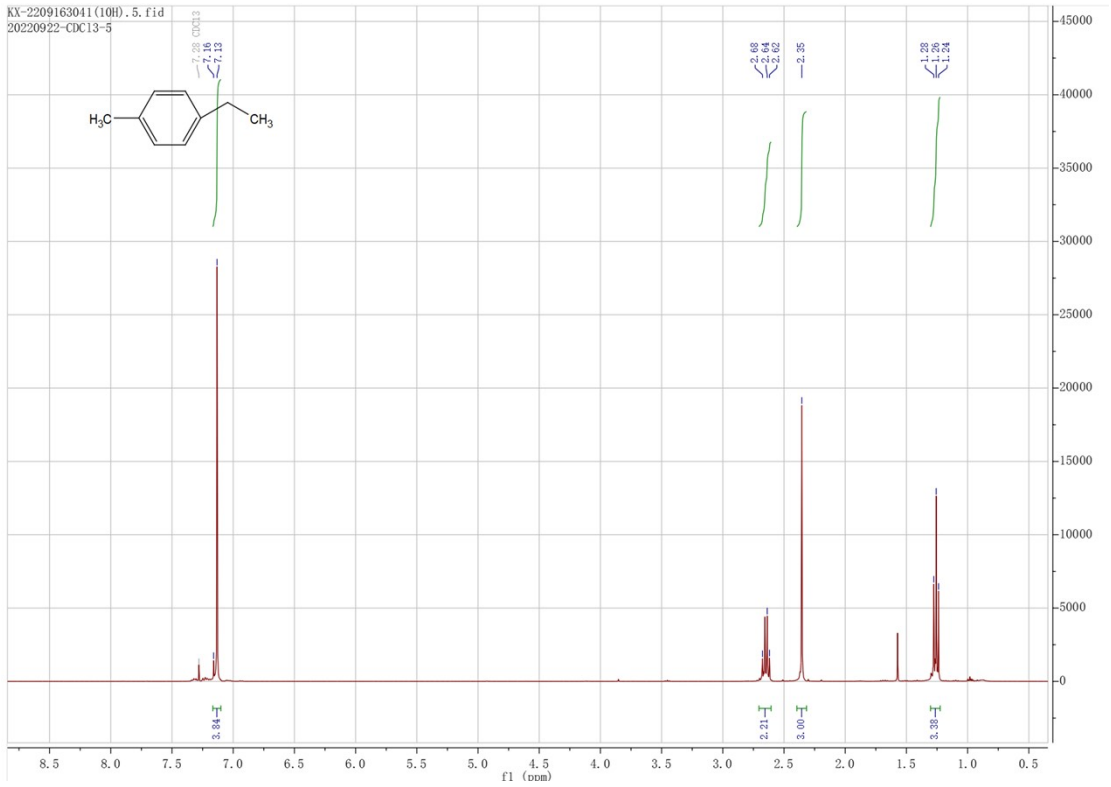

^{1}H NMR (500 MHz, $CDCl_3$): δ (ppm): 7.16-7.13 (d, 4H), 2.68-2.62 (m, 2H), 2.35 (s, 3H), 1.28-1.24 (m, 3H).

Figure S13. The GC-MS and ^{1}H NMR spectrum of the hydrogenation results (table 2 of main text, entry 6).

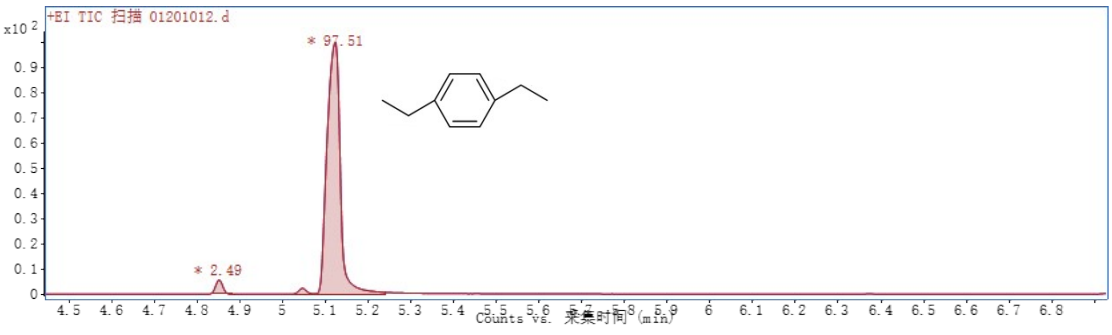

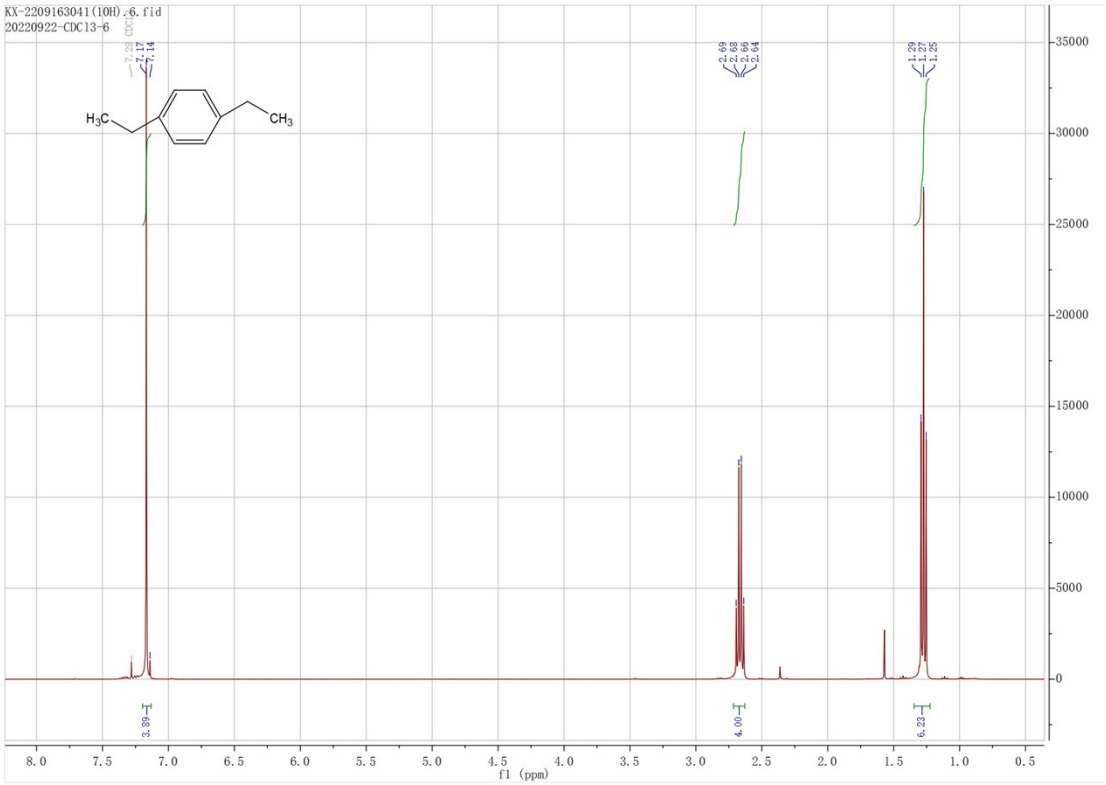

146

147 ^{1}H NMR (500 MHz, $CDCl_3$): δ (ppm): 7.17-7.14 (d, 4H), 2.69-2.64 (m, 4H), 1.29-

148 1.25 (m, 6H).

149 **Figure S14.** The GC-MS and ^{1}H NMR spectrum of the hydrogenation results (table 2

150 of main text, entry 7).

151

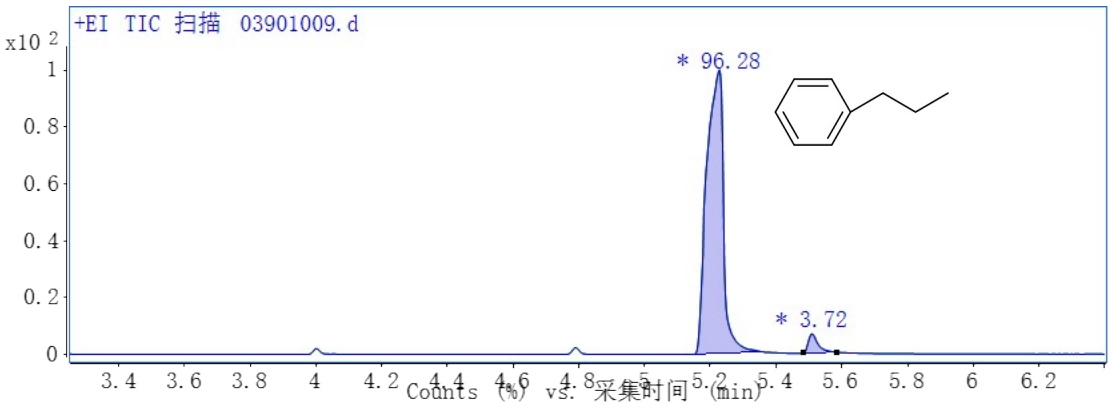

152

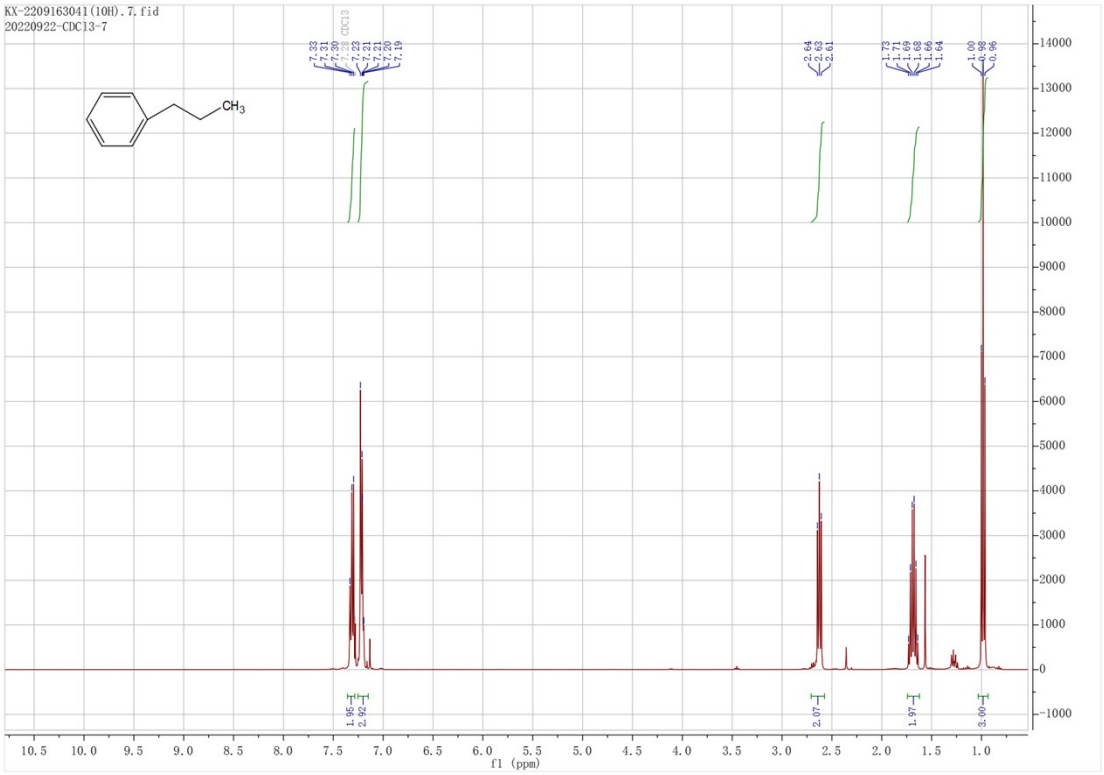

153

154 ^{1}H NMR (500 MHz, $CDCl_3$): δ (ppm): 7.33-7.31 (m, 2H), 7.23-7.19 (m, 3H), 2.64-

155 2.61 (t, 2H), 1.73-1.64 (m, 2H), 1.00-0.96 (t, 3H).

156 **Figure S15.** The GC-MS and ^{1}H NMR spectrum of the hydrogenation results (table 2

157 of main text, entry 8).

158

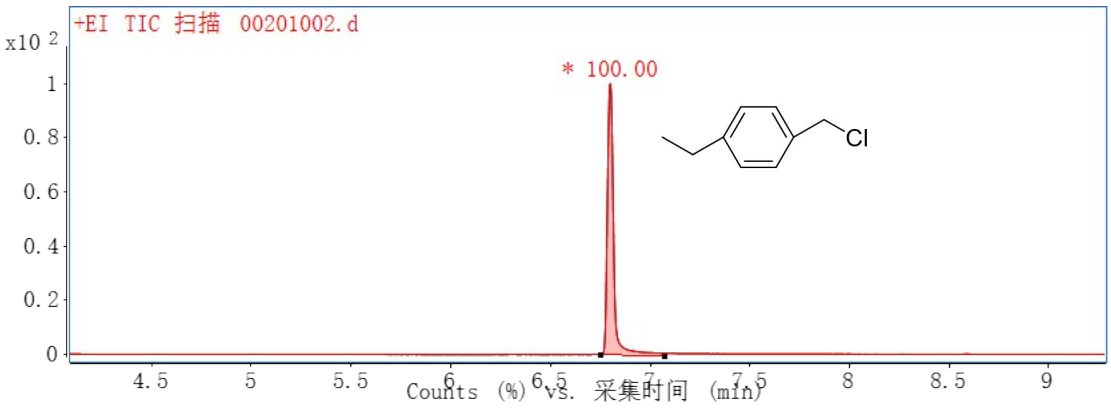

159

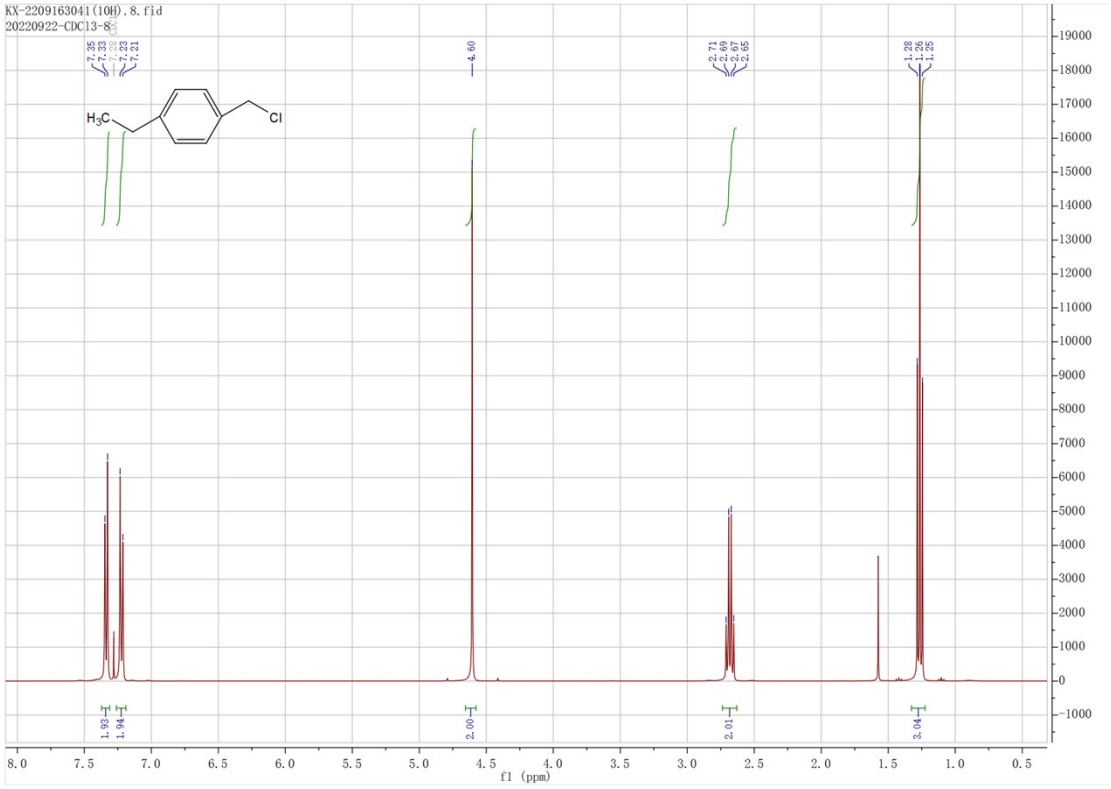

[1]H NMR (500 MHz, $CDCl_3$): δ (ppm): 7.35-7.33 (d, 2H), 7.23-7.21 (d, 2H), 4.60 (s, 2H), 2.71-2.65 (m, 2H), 1.28-1.25 (t, 3H).

Figure S16. The GC-MS and [1]H NMR spectrum of the hydrogenation results (table 2 of main text, entry 9).

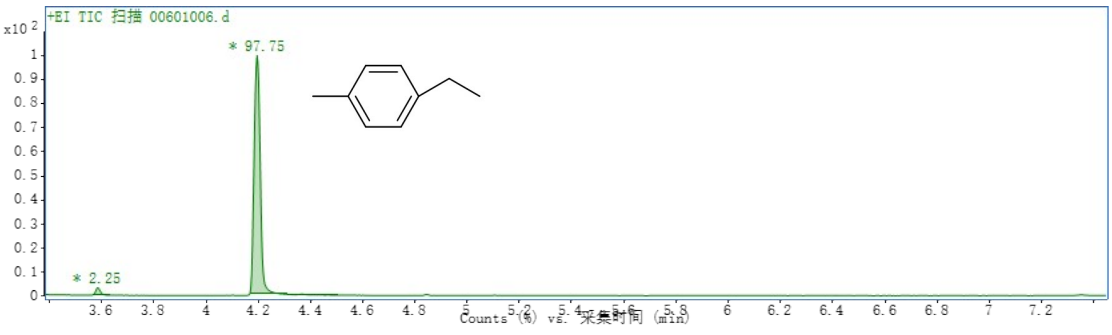

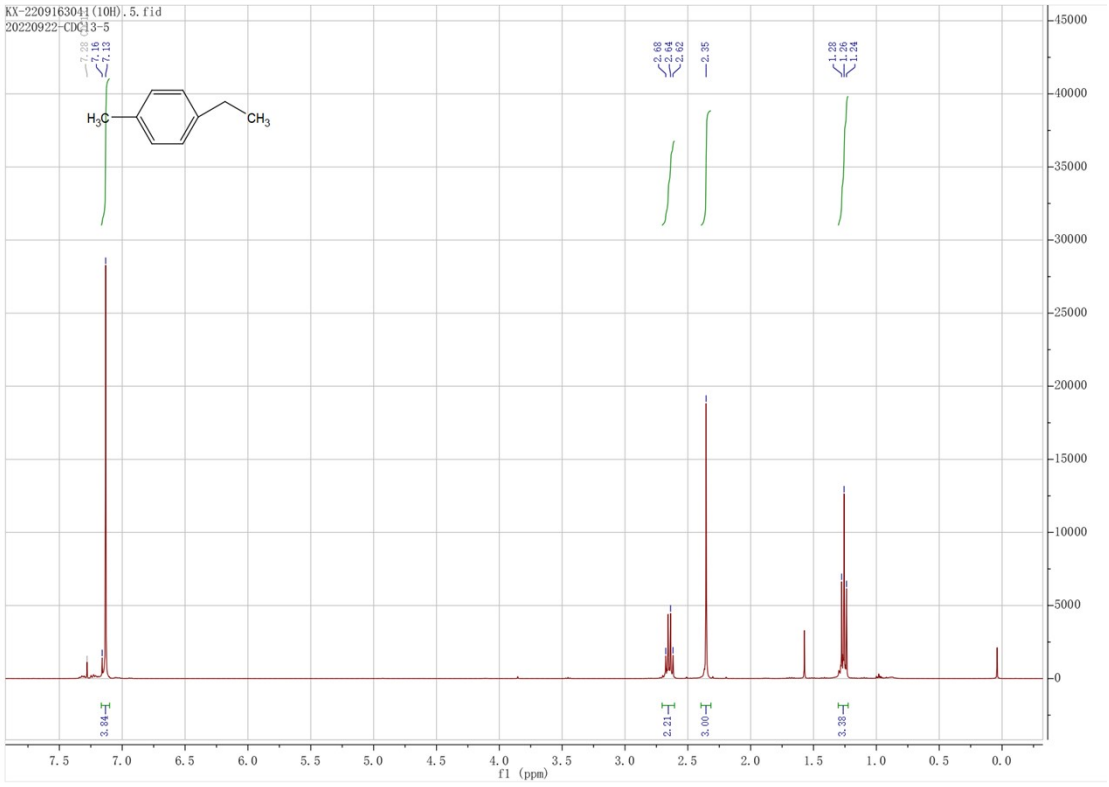

[1]H NMR (500 MHz, $CDCl_3$): δ (ppm): 7.16-7.13 (d, 4H), 2.68-2.62 (m, 2H), 2.35 (s, 3H), 1.28-1.24 (t, 3H).

Figure S17. The GC-MS and [1]H NMR spectrum of the hydrogenation results (table 2 of main text, entry 10).

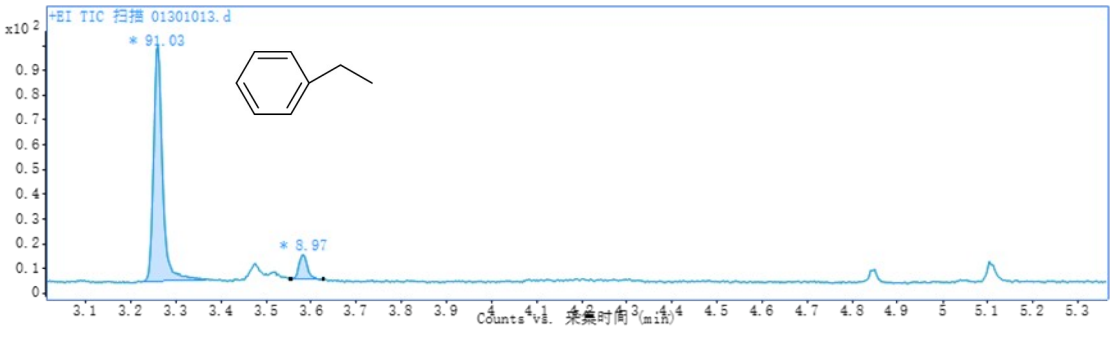

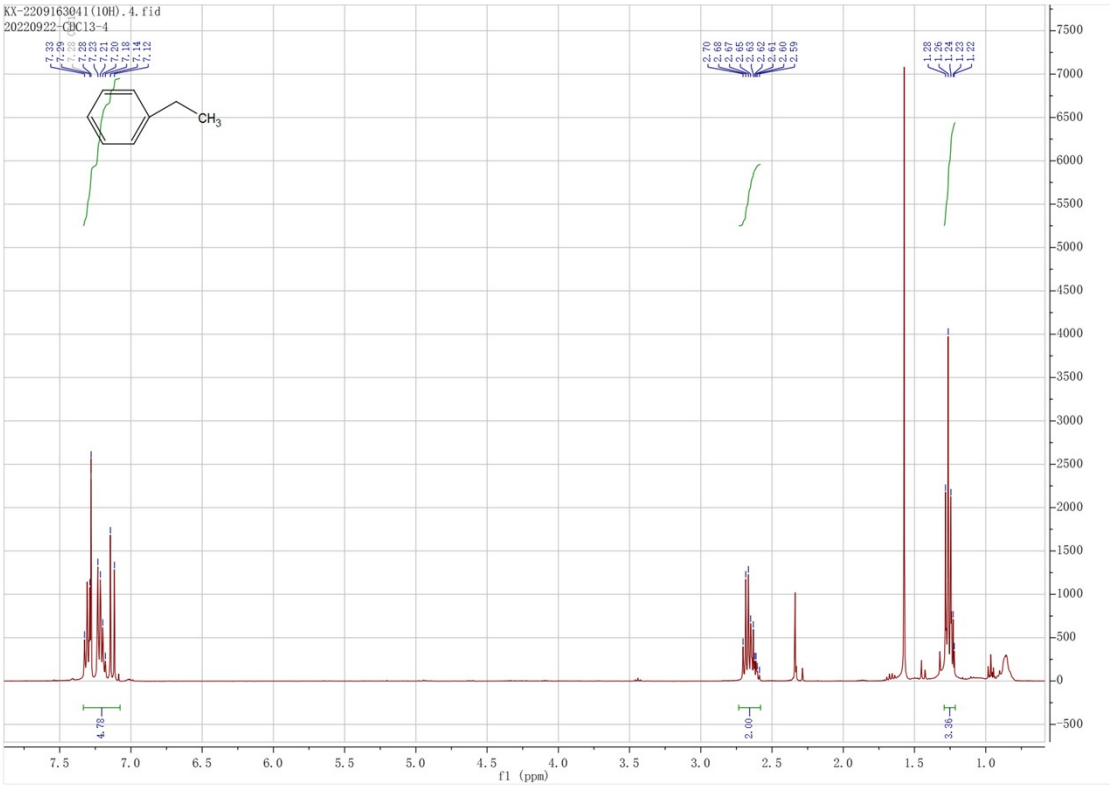

174

175 ^{1}H NMR (500 MHz, $CDCl_3$): δ (ppm): 7.33-7.12 (m, 5H), 2.70-2.59 (m, 2H), 1.28-

176 1.22 (m, 3H).

177 **Figure S18.** The GC-MS and ^{1}H NMR spectrum of the hydrogenation results (table 2

178 of main text, entry 11).

179

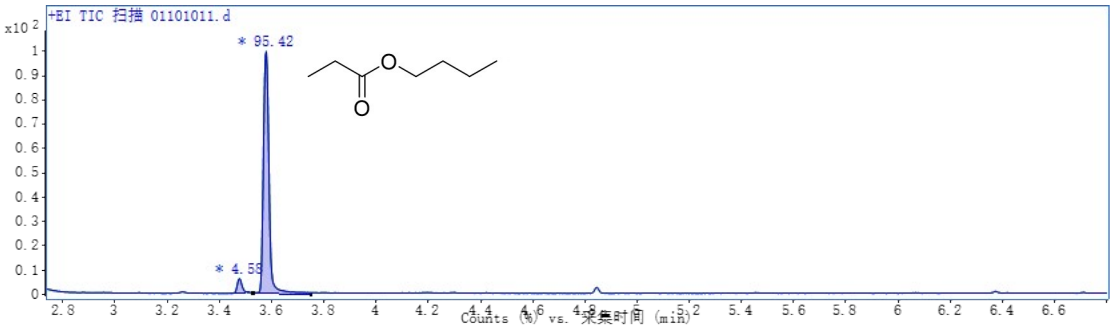

180

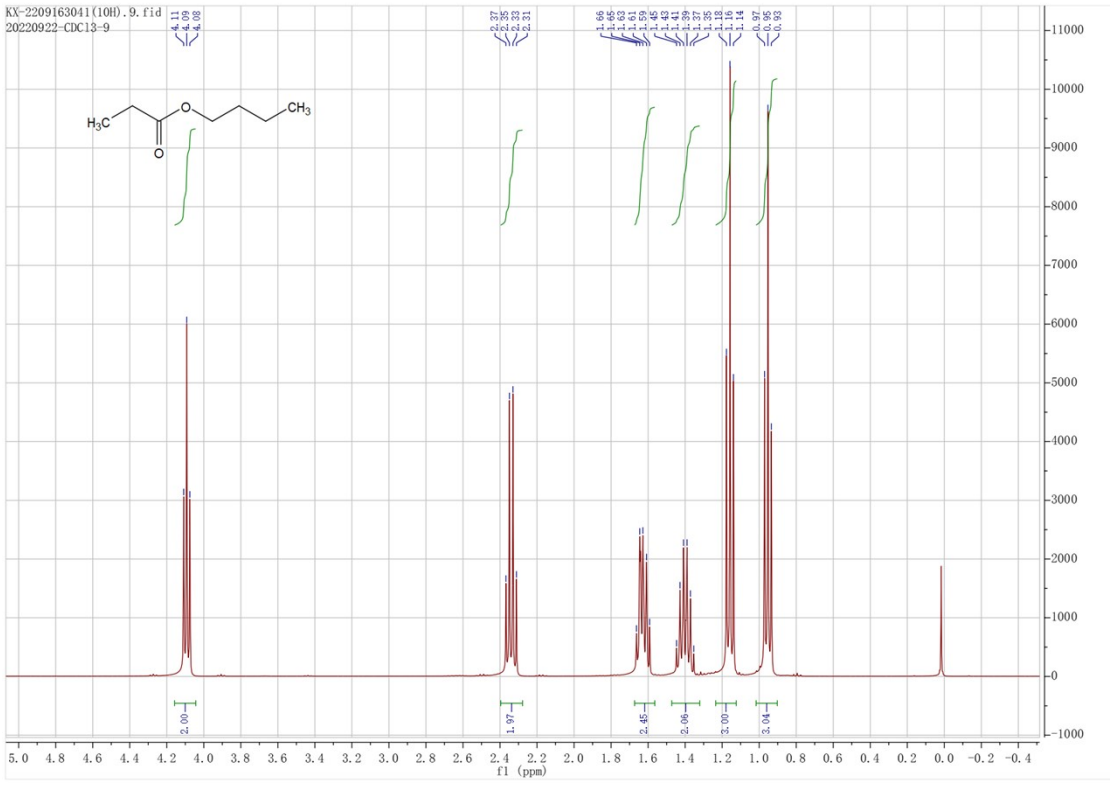

181

182 ^{1}H NMR (500 MHz, $CDCl_3$): δ (ppm): 4.11-4.08 (t, 2H), 2.37-2.31 (m, 2H), 1.66-1.59

183 (m, 2H), 1.45-1.35 (m, 2H), 1.18-1.14 (t,3H), 0.97-0.93 (t, 3H).

184 **Figure S19.** The GC-MS and ^{1}H NMR spectrum of the hydrogenation results (table 2

185 of main text, entry 12).

186

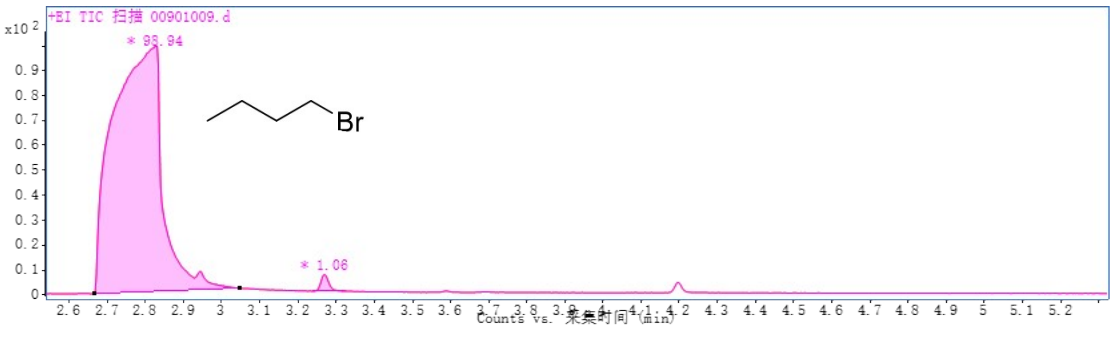

187

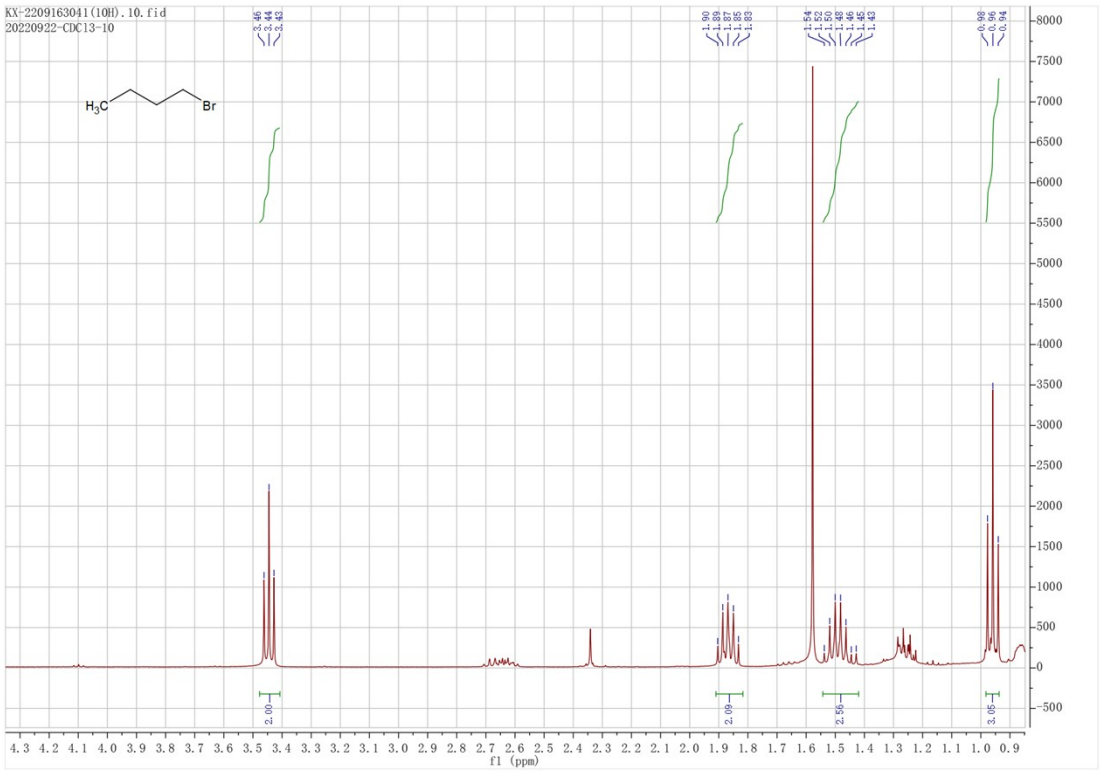

^{1}H NMR (500 MHz, $CDCl_3$): δ (ppm):3.46-3.43 (t, 2H), 1.90-1.83 (m, 2H), 1.54-1.43 (m, 2H), 0.98-0.94 (t, 3H).

Figure S20. The GC-MS and ^{1}H NMR spectrum of the hydrogenation results (table 2 of main text, entry 13).

Reference.

1. Z. Li, Y. Shi, A. Zhu, Y. Zhao, H. Wang, B. P. Binks and J. Wang, Angew Chem Int Ed Engl, 2021, 60, 3928-3933.

2. L. Fu, S. Li, Z. Han, H. Liu and H. yang, Chem Commun (Camb), 2014, 50, 10045-10048.

3. J. Huang and H. Yang, Chem Commun (Camb), 2015, 51, 7333-7336.

4. F. Harraz, S. El-Hout, H. Killa and I. Ibrahim, Journal of catalysis, 2012, 286, 184-192.